

Electrochemical and mass measurements during small voltage amplitude perturbations of conducting polyaniline films

Huyen N. Dinh, Viola I. Birss *

Department of Chemistry, University of Calgary, Calgary, Alberta, Canada T2N 1N4

Received 20 February 1997; received in revised form 12 August 1997

Abstract

The electrochemistry of conducting polyaniline (PANI) films has been studied in sulfuric acid solutions using a.c. impedance and cyclic voltammetry (CV), coupled with the quartz crystal microbalance (QCMB) technique. In normal full potential range slow sweep CV experiments, the fact that the mass-to-charge ratio increases markedly with potential in the positive scan, but is essentially constant during the negative scan, may be related to slow water penetration into the film during its oxidation. When only small potential amplitudes of ca. 25 mV or less are employed, the CV and QCMB measurements reveal that additional film sites can be initially oxidized, but not reduced, unless the potential is made more negative. This leads to an apparent loss in film capacitance when only narrow potential ranges are cycled. These results, together with increased hysteresis in the mass response with increasing sweep rate as well as the known asymmetries of the PANI CV response, suggest that given enough time, water can penetrate the film, hydrating some of the reduced PANI sites and facilitating their oxidation but not their reduction. The subsequent steady-state but lowered film capacitance must reflect the reversible oxidation/reduction of film sites which are not susceptible to delayed water transport and/or the stabilizing effects due to site hydration. © 1998 Elsevier Science S.A.

Keywords: Polyaniline; Impedance; Capacitance; Quartz crystal microbalance; Ion compensation; Hysteresis behavior

1. Introduction

It is relatively well known that when the capacitance of certain electrochemically formed polymer films, e.g., polyaniline (PANI), is determined in their conducting state by impedance techniques, the measured capacitance is often substantially lower than that predicted from the cyclic voltammetric (CV) response [1–9], i.e., from the current divided by the sweep rate. It has been suggested that this lower capacitance [9] is not a kinetic effect but is the direct consequence of the perturbation of the film by comparatively small voltage amplitudes (typically 5 to 10 mV in impedance experiments). A wide potential range (e.g., 0 to 0.6 V) must be used to interconvert these films between the fully insulating and conducting states in cyclic voltammetry experiments.

Ren and Pickup [9] have shown that when the potential is swept over a 10 mV range in a CV experiment involving a poly[1-methyl-3-(pyrrole-1-ylmethyl) pyridinium] (poly-

MPMP⁺) film, the capacitance was only ca. 70% of that obtained from a full CV sweep over a range of 550 mV. They also showed that the extent of capacitance loss is not kinetic in origin, as the time scale of the a.c. impedance experiment was longer than that in the CV experiments, but that it was dependent only on the amplitude of the potential perturbation employed. It was suggested [9] that this amplitude dependence of the capacitance loss is an indication that only certain polymer sites can change their conformation from the planar form of the oxidized PANI to the twisted form of the reduced film, and back, over a narrow potential range. Therefore, for small potential amplitudes, only a fraction of the polymer sites can react.

The overall goal of the present work has been to examine more closely the electrochemistry of the conducting form of PANI when a small amplitude perturbing voltage, such as is employed in a.c. impedance experiments, is utilized. As part of this, a deeper understanding of the origin and significance of the apparent loss of film capacitance, observed under these conditions, has been sought. To accomplish these goals, experiments were designed to monitor the overall mass change of PANI films,

* Corresponding author. Tel.: +1-403-220-6432; fax: +1-403-289-9488; e-mail: birss@acs.ucalgary.ca.

as well as any changes in the mass gain/loss associated with the injection/expulsion of charge compensating electrolyte ions, as a function of the amplitude of the perturbing voltage and the sweep rate. These results have been compared with the mass changes measured over the same narrow potential ranges (e.g., 25 mV) during full potential range CV scans. The impedance and CV responses were also examined in this work.

2. Experimental

Cyclic voltammetry (CV) was performed using EG&G PARC 173/175 instrumentation. The a.c. impedance measurements were carried out with a Solartron 1255 frequency response analyzer connected to a Solartron 1286 electrochemical interface. The impedance instruments were programmed and data collection was performed using Z-Plot software (Scribner Associates). Impedance data were obtained at a fixed dc potential, ranging from 0.2 to 0.8 V vs. RHE, normally using a 10 mV rms potential amplitude and frequencies from 0.1 to 100 kHz. The PANI film capacitance was obtained from the constant phase element, CPE, by fitting the data (with emphasis on the low frequencies) to a simple series R-CPE circuit using a computer best-fit method (EQUIVCRT, B. Boukamp).

Quartz crystal microbalance (QCMB) experiments were carried out using a home-made oscillator (Pierce type), connected to a Philips PM 6654C programmable high resolution frequency counter. The resonant frequency of the oscillating PANI-coated quartz crystal was measured in situ as a function of potential. For this study, QCMB and CV responses were recorded simultaneously over a range of voltage amplitudes (25, 50, 100, and 600 mV), using sweep rates of 2 to 20 mVs⁻¹.

Standard three-electrode, two-compartment cells were used for PANI growth, QCMB, and a.c. impedance measurements. The working electrode (WE) for a.c. impedance and standard CV measurements was a polycrystalline gold wire (Aldrich, 99.99%, 0.5 mm diameter), embedded in soft glass tubing. For QCMB experiments, the WE was an AT-cut quartz crystal (Valpy–Fisher, 5 MHz, 2.5 cm diameter), sputter coated first with a thin film of titanium for adherence and then a thin film of gold. The crystal constant was 56.6 Hz cm² µg⁻¹, according to the Sauerbrey equation [10]. The counter electrode (CE) was a large area Pt gauze and the reference electrode (RE) was a reversible hydrogen electrode (RHE). For impedance measurements, a fourth, pseudo-reference electrode (a platinum gauze) was placed in the WE compartment and was electrically connected to the RE via a 6.8 µF capacitor to avoid artifactual phase shifts at high frequencies.

All data in this paper are reported versus the RHE. All CV and QCMB data are given with respect to the geometric electrode area. Only the capacitance data are given with respect to the real electrode area, which was determined

from the comparison of the measured gold oxide formation/reduction charge with the literature value (400 µCm⁻²) [11].

Both aniline (Fischer Scientific, Certified ACS) and sulfuric acid (BDH, ACS Assured, 95.0%–98.0% assay) were used as received. All solutions were prepared with triply distilled water. All experiments were carried out at room temperature. Solutions were deaerated by purging nitrogen either through or above the cell solution during all of the experiments.

PANI films were grown on a polycrystalline gold wire WE by cycling at 100 mVs⁻¹, or on gold-sputtered quartz crystals at 50 mVs⁻¹, between 0.00 V and 1.05 V vs. RHE for the first few cycles and then between 0.00 V and +0.95 V for subsequent cycles in 0.1 M aniline + 1 M H₂SO₄ solution for 1 to 2 h. The PANI-coated gold WEs were then transferred to a fresh, deoxygenated 1 M H₂SO₄ solution to examine the CV, QCMB, and a.c. impedance responses. The PANI film thickness was estimated using the published relationship of 800 Ccm⁻³, using the measured anodic PANI charge obtained from slow sweep CVs between 0.00 V and +0.80 V vs. RHE [12].

3. Results and discussion

3.1. Capacitance loss during impedance measurements

Fig. 1 (curve a) shows a typical CV (100 mVs⁻¹), with the current given in units of capacitance (*j*/s), of a PANI

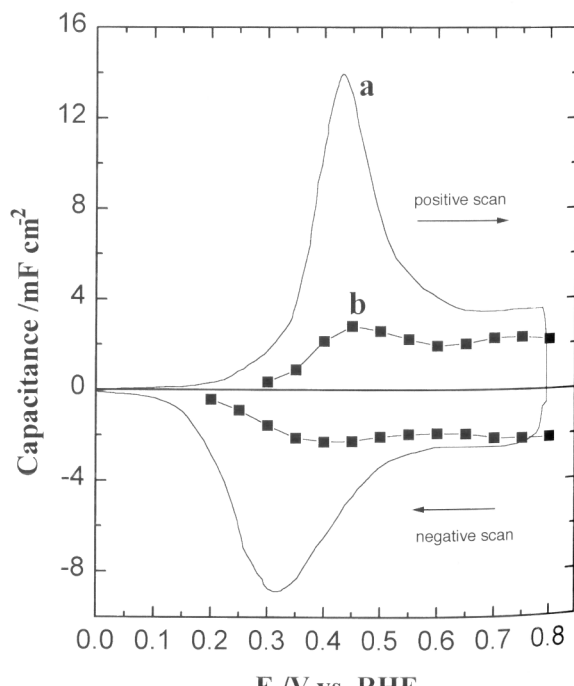


Fig. 1. Plot of (a) CV-determined capacitance (*j*/s) (*s* = 100 mVs⁻¹) and (b) impedance-determined film CPE as a function of potential for a 35 nm PANI film in 1 M H₂SO₄ solution.

film, estimated to be 35 nm in thickness [12], formed on a Au wire substrate. As the PANI film is still thin, there are no mass transport limitations and all of the CV currents are linearly proportional to sweep rate. Curve b shows the impedance-determined capacitance of the film at various potentials using a rms voltage amplitude of 10 mV, and a frequency range of 0.1 to 10 Hz (a similar time domain as used in the CV experiments). This frequency range is used as it is only at these low frequencies that the purely capacitive response of PANI films is seen. The raw impedance data collected in the present work are very similar to those published previously, and readers are therefore referred to the prior relevant literature [1–8] in order to examine typical raw impedance data for PANI films.

It is notable that, while the capacitance is measured as a constant phase element (CPE), a CPE can be considered to be equivalent to a capacitance when the ‘*n*’ exponent is very close to unity, as was the case here (0.97 ± 0.01). The impedance-determined capacitance is seen in Fig. 1 to be ca. 55 to 85% of the CV capacitance at potentials between 0.6 and 0.8 V, but much less, ca. 20 to 25% of the CV capacitance, in the potential range of the peaks. This phenomenon, similar to what has been reported by Kalaji and Peter [8], has been found to be essentially independent of PANI film thickness and of sweep rate in our experiments. It is the main purpose of this paper to provide insight into the origin of this apparent loss of capacitance in impedance experiments, primarily through the use of in situ mass measurements, as follows.

3.2. Mass change analysis as a function of potential in full range CV experiments

The monitoring of mass changes as a function of potential amplitude was suggested in an earlier publication [8] as a promising experiment to attempt in order to provide further understanding of the capacitance loss in small voltage amplitude vs. full range CV experiments. To aid in the interpretation of the mass data obtained in such experiments, a careful analysis of the mass changes measured over distinct potential intervals during a full potential sweep was first carried out. Fig. 2 (curves a and b) show two typical large voltage amplitude CVs (5 mVs^{-1}) from 0 to 0.6 V and to 0.45 V, respectively, for a PANI film (ca. 80 nm) on a Au/quartz crystal substrate. Fig. 3 (curves a and b) shows the corresponding frequency-potential responses for these two large amplitude CVs (600 mV and 450 mV). Mass gain (loss), i.e., frequency decrease (increase), is observed during PANI oxidation (reduction), similar to numerous prior reports in the literature [13–20]. The sweep rates employed in all of these experiments were made sufficiently slow so that no transport limitations are present and all PANI sites can react (currents and charges are all linearly proportional to sweep rate at all potentials, as shown in Fig. 4).

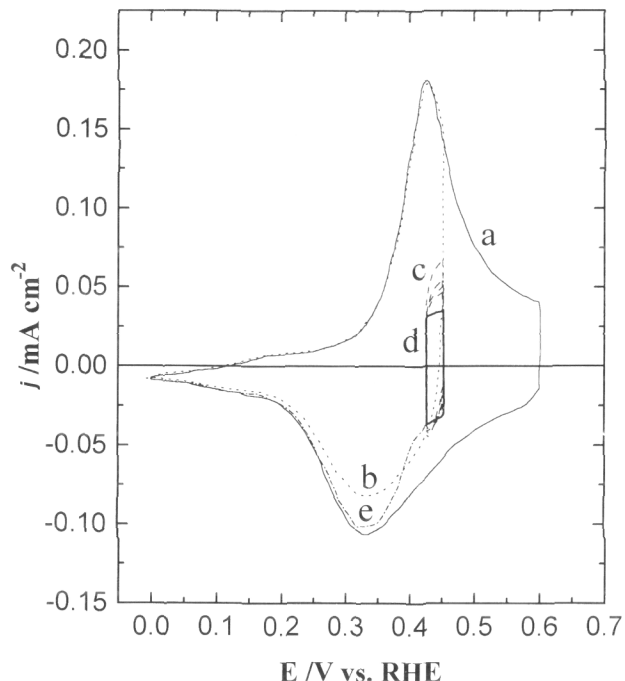


Fig. 2. CV responses (5 mVs^{-1}) in $1 \text{ M H}_2\text{SO}_4$ for an 80 nm thick PANI film, deposited on a Au quartz crystal substrate, scanned between (a) 0 and 0.6 V (—), (b) 0 and 0.45 V (· · ·), (c) multicycled between 0.425 and 0.450 V (---), (d) steady state response between 0.425 and 0.450 V (—), and then scanned negatively to 0 V (— · —).

In preparation for the analysis of the mass change data in the small voltage amplitude experiments, these normal full scale CVs between 0 and 0.6 V were analyzed in detail in 25 mV segments to determine the mass-to-charge ratios as a function of dc potential. This was done by integrating the charge passed and measuring the corresponding mass change over each 25 mV interval throughout each single full cycle of potential. These two measurements were made over a range of sweep rates for which the linear relationship of Fig. 4 pertained. Table 1 gives these mass-to-charge ratios for 5 mVs^{-1} scans in both the positive and negative directions. In the positive scan, the ratios are initially relatively small, i.e., $10 \text{ to } 15 \text{ g(mol e}^{\text{-}}\text{)}^{-1}$. The ratio gradually increases to ca. $45 \text{ g(mol e}^{\text{-}}\text{)}^{-1}$ when the PANI film is fully conducting at more positive potentials. In the negative scan, the ratio is much more constant with potential, being approximately $30 \text{ g(mol e}^{\text{-}}\text{)}^{-1}$.

It has been suggested previously [16,18,20,21] that charge compensation during PANI oxidation (reduction) is achieved by a mixture of proton expulsion (injection) and bisulfate or sulfate injection (expulsion) in sulfuric acid solutions. In the predominantly reduced form of PANI, charge compensation is achieved primarily by protons [13,15,17,18,21], consistent with the lower mass-to-charge ratios observed. The ratio of $10 \text{ to } 20 \text{ g(mol e}^{\text{-}}\text{)}^{-1}$ in the early part of the positive scan would be consistent with ca. 1 mole of bisulfate ions being injected and 3 moles of hydrated protons being expelled for every 4 moles of

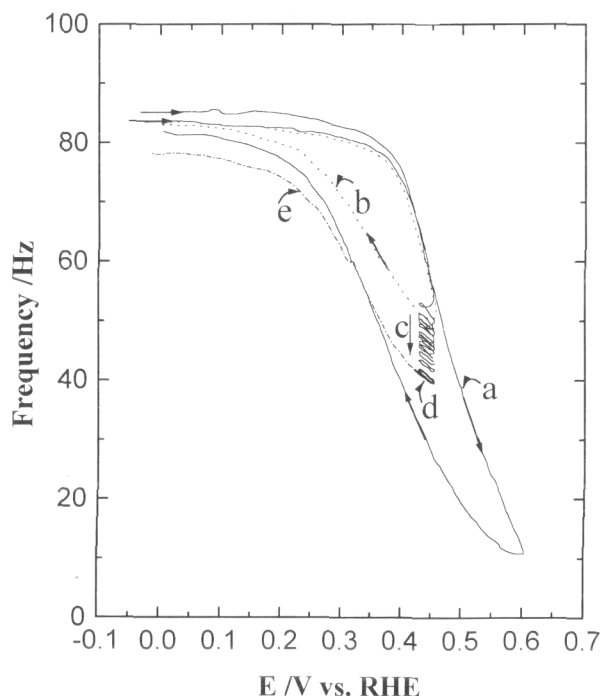


Fig. 3. The effect of sweep rate on the anodic currents at various potentials: 0.45 V (■), 0.50 V (●), 0.55 V (▲), and 0.575 V (×), for an 80 nm thick PANI film, deposited on a Au quartz crystal substrate, in 1 M H₂SO₄.

electrons removed from the film. At higher potentials, sulfate ions are believed to be the majority charge compensating species, in agreement with the higher ratios (higher masses) observed. Indeed, if charge compensation were accomplished only by sulfate injection during oxidation, then the observed mass-to-charge ratio should be 48 g(mol e⁻)⁻¹, similar to what is seen in Table 1 at 0.575 V. Sulfate is the species considered at more positive potentials, as it is reasonable that it would be stabilized (vs. bisulfate), since the proton content of the film is now expected to be quite low. The relatively constant ratio of ca. 30 g(mol e⁻)⁻¹ seen in the negative scan would then suggest a more uniform ratio of protons injected to sulfate ions expelled. However, it is clear that there is no single interpretation of any of these mass-to-charge ratios, especially when free water may also be injected and expelled during potential cycling. This ambiguity appears to be consistent with the absence of an agreed upon charge compensation mechanism for PANI in the prior literature [18,20,22].

Despite this, however, several interesting observations emerge from this data. The fact that the anodic ratios increase with potential, while the cathodic ratios are essentially constant during PANI reduction, shows that differences in the PANI oxidation and reduction processes do exist. Perhaps this is not surprising, considering that the anodic and cathodic CV profiles are clearly asymmetrical, as has been pointed out previously by others [23–25]. For

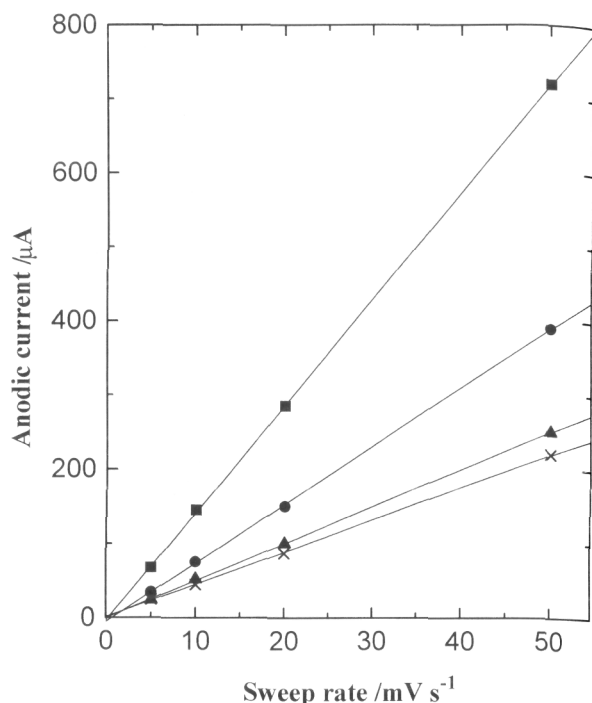


Fig. 4. The frequency-potential response corresponding to the CVs in Fig. 2 for an 80 nm thick PANI film deposited on Au quartz crystal substrate, scanned between (a) 0 and 0.6 V (—), (b) 0 and 0.45 V (· · ·), (c) multicycled between 0.425 and 0.450 V (—), (d) steady state response between 0.425 and 0.450 V (—), and then reduced to 0 V (— · —).

example, even though all currents are linearly proportional to sweep rate (Fig. 4) under the conditions used in this work, the anodic peak is always notably sharper and narrower than the cathodic peak. Also, there is a persistent (constant) difference in the anodic and cathodic peak potentials, despite the fact that they are each independent of sweep rate. It has been argued by Feldberg and Rubenstein [23] that this is consistent with the properties of an N-shaped Gibbs energy curve, and that some rate processes (but not electron or charge compensating ion trans-

Table 1

Ratio of mass change to charge passed, determined by analysis of a single CV between 0 and 0.6 V ($s = 5 \text{ mVs}^{-1}$) (curve a of Fig. 2 and Fig. 3) in 25 mV segments

Potential range/V (vs. RHE)	Mass to charge ratio/g(mol e ⁻) ⁻¹ Positive scan	Negative scan
0.325 ↔ 0.350	11	-21
0.350 ↔ 0.375	13	-25
0.375 ↔ 0.400	15	-27
0.400 ↔ 0.425	16	-27
0.425 ↔ 0.450	19	-30
0.450 ↔ 0.475	29	-29
0.475 ↔ 0.500	35	-31
0.500 ↔ 0.525	38	-32
0.525 ↔ 0.550	43	-27
0.550 ↔ 0.575	43	-25

Under the negative scan column, the negative sign indicates mass loss, i.e., net expulsion of ions, during film reduction.

port) must be slow on the time scale of observation in order for this steady-state hysteresis to be observed (termed the ‘unusual quasi reversibility’ (UQR) condition). Some possible slow chemical processes which could apply include ion pairing of the charge compensating anions with fixed polymer cationic sites, polymer site hydration and conformational changes of the PANI film. Some examples of the latter include rearrangement of the polymer chain configuration, producing open and closed channels [24], and a change in the polymer chains from planar to twisted, and vice versa, with oxidation/reduction of PANI films [25].

The fact that the anodic currents are larger than the cathodic ones at every potential in the range from ca. 0.4 to 0.6 V (curve a in Fig. 2), even while a linear current–sweep rate relationship exists at these potentials (Fig. 4), is also interesting. This is consistent with the observation that, when the positive scan is reversed at any potential within this range, the cathodic current is always lower than the corresponding anodic current was at the same potential. Apparently, only some fraction of film sites can be reversibly reduced and oxidized over any potential range. As this cannot be related to slower charge transfer during reduction vs. oxidization, based on Fig. 4, it may be another characteristic of systems exhibiting UQR [23].

The marked increase of the anodic ratios with increasing potential, while the cathodic ratios appear to be comparatively constant, could imply that steady-state conditions exist throughout the film during its reduction, whereas the film properties are changing continuously with increasing potential during oxidation, at least from 0.3 to 0.55 V. This difference may reflect a different spatial distribution of oxidized and reduced sites in the two cases. For example, as PANI oxidation commences at the Au/polymer interface [4,26], it is possible that the reaction front moves as a planar boundary towards the film|solution interface. In this case, the lower initial anodic mass-to-charge ratios would then represent more protonic charge compensation as sites deep within the nonconducting PANI film react, while the higher anodic ratio at more positive potentials would reflect the oxidation of outer film sites with simultaneous sulfate injection. Alternatively, oxidation may occur along individual polymer chains, starting with the sites closest to the metal surface and extending to those nearer to the polymer|solution interface as the potential increases. The reduction of PANI, now in its conducting state and perhaps altered quite significantly in composition and/or structure by the slow chemical process implied by the UQR condition [23], may occur in a more random manner throughout the film, thus retaining spatially more homogeneous film properties.

Another possibility is that these differences in the PANI film oxidation and reduction CV characteristics and the mass-to-charge ratios are related to pH gradients which develop within the film, particularly during the oxidation step. As proton expulsion occurs during oxidation and the

inner PANI sites experience an increasing local pH, the outer regions of the film would continue to be influenced by the acidity of the external H_2SO_4 solution. In contrast, proton injection into the fully conducting PANI film, which is likely to occur first at the outer film|solution interface, may lead to a more homogeneous internal film pH.

It seems even more likely that the differences in the anodic and cathodic ratios shown in Table 1 reflect differences in the potential (or time, or PANI state) dependence of the injection and expulsion of water during oxidation vs. reduction. In the positive sweep, the high ratios observed at more positive potentials, when sulfate ions are believed to be injected, might also reflect the co-injection of water. At less positive potentials, when the lowest ratios are observed, less water would enter the film while protons are being expelled. During reduction, water would then appear to be expelled in a more uniform manner, based on the fact that the mass-to-charge ratio has an intermediate and essentially constant value.

In support of these suggested asymmetries in water transport with sweep direction and potential, it was observed that increasing the sweep rate (while still maintaining the linear current–sweep rate relationship condition) results in a greater hysteresis in the mass response (Fig. 5). Even while a constant total mass change (70 ± 2 Hz) is still seen, the maximum film mass is observed only after film reduction is well underway at the higher sweep rates. Since the electrochemistry continues to be kinetically unhindered and unchanged, the delayed mass transport must

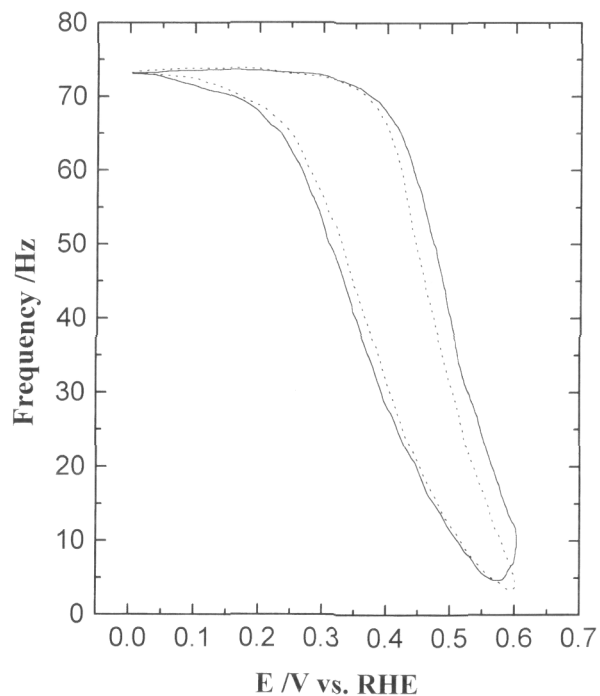


Fig. 5. Mass changes as function of potential, scanned at 50 mVs^{-1} (—) and 10 mVs^{-1} (· · ·) for an 80 nm thick PANI film, deposited on a Au quartz crystal substrate, in $1\text{ M }H_2SO_4$.

be that of a neutral species, suggested here to be the solvent, water. Particular difficulties associated with electroactive polymer ‘break-in’ [27–29], i.e., the conversion of polymer films from their more shrunken (reduced) to swollen (oxidized) states, have been reported previously [13,30,31]. The injection (expulsion) of water into PANI during film oxidation (reduction) is suggested below to be related to some of the unusual aspects of PANI electrochemistry when small voltage amplitudes are employed.

3.3. Mass measurements during small voltage amplitude experiments

The principal goal of the subsequent set of experiments was to compare the mass-to-charge ratios obtained in the full potential range CV experiments described above (Table 1) with those measured during narrow voltage (25 mV) amplitude excursions at 5 mVs^{-1} and centered at potentials at which PANI is conducting, i.e., 0.40 to 0.55 V. Curves c in Fig. 2 demonstrate the electrochemical response observed during multicycling between the potential limits of 0.425 and 0.450 V. Of immediate interest is the fact that in each of the 5 to 10 cycles leading to steady-state, the overall anodic charge passed is larger than the cathodic, with the difference between them decreasing with cycling time until the steady-state, symmetrical response of curve d (Fig. 2) is seen. This shows that, surprisingly, additional PANI sites can be oxidized but they cannot be reduced when only the narrow potential range of 25 mV is traversed. Indeed, when the lower limit is extended to its usual value of 0.0 V in the following full negative scan (curve e of Fig. 2), the cathodic counterpart to the excess anodic charge passed in curves c (Fig. 2) is now seen (note that a larger cathodic charge is now passed than in the normal full scan from 0.45 V in curve b of Fig. 2). As this experiment was carried out at a very slow sweep rate and as the same observations were seen at 10 and 20 mVs^{-1} (all currents are still linearly proportional to sweep rate), this capacitance loss and the observed oxidation (but not reduction) of additional PANI sites are not due to slow electron or ion transfer effects. It appears that spending time in a narrow range of potential (or at a constant potential, as seen in other parallel experiments) can cause a change in film properties, such that sites normally not oxidizable in a full slow sweep CV scan until higher potentials are attained, can now react. This is an unusual observation and may again be a characteristic of a system exhibiting UQR behavior [23].

One possible explanation for this, based on the notion of delayed water injection during film oxidation (Fig. 5), is that sufficient time is now provided for water to penetrate the film, hydrating some initially reduced PANI sites so that they can now be oxidized. The stabilization of these newly oxidized sites by hydration is consistent with the more negative potential that must then be applied to reduce them. An examination of the mass change of the film

during the time of cycling between 0.425 and 0.450 V yields a relatively high mass-to-charge ratio of ca. $40 \text{ g}(\text{mol e}^-)^{-1}$, similar to that seen at potentials of ca. 0.5 V or higher (Table 1), where it was ascribed to both sulfate and water injection.

To ascertain whether the PANI sites which were oxidized, but not reduced in curves c, reflect sites which would normally have reacted at more positive potentials, or whether they might represent additional sites which are not accessible in a normal full potential range CV, the following experiment was carried out. The PANI film was cycled within a narrow potential range, i.e., between 0.425 and 0.450 V, until a steady-state, symmetrical CV response such as in curve d (Fig. 6) was seen. The potential was then scanned positively to 0.60 V and then back to 0 V. It can be seen in Fig. 6 that less anodic charge is passed from 0.45 to 0.60 V than in a normal full positive scan, suggesting that some of these sites have reacted already during the time of multicycling between 0.425 and 0.450 V. The fact that a similar cathodic charge is passed in the next reduction scan, as compared to that in a typical full potential range CV, indicates that only those sites which normally react in slow sweep CVs are involved in these experiments. These results further confirm that the excess anodic charge passed in the time of cycling over the narrow potential range (25 mV) reflects the oxidation of PANI sites which would normally have been able to react only at more positive potentials. To reiterate, it is suggested that

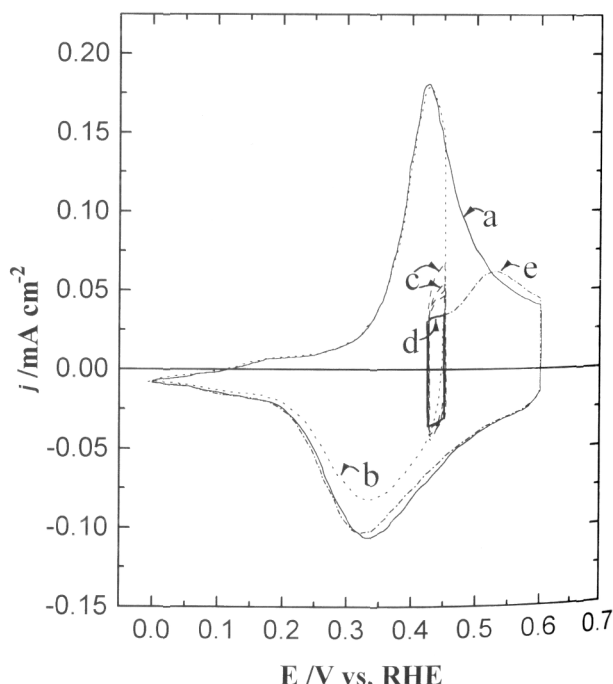
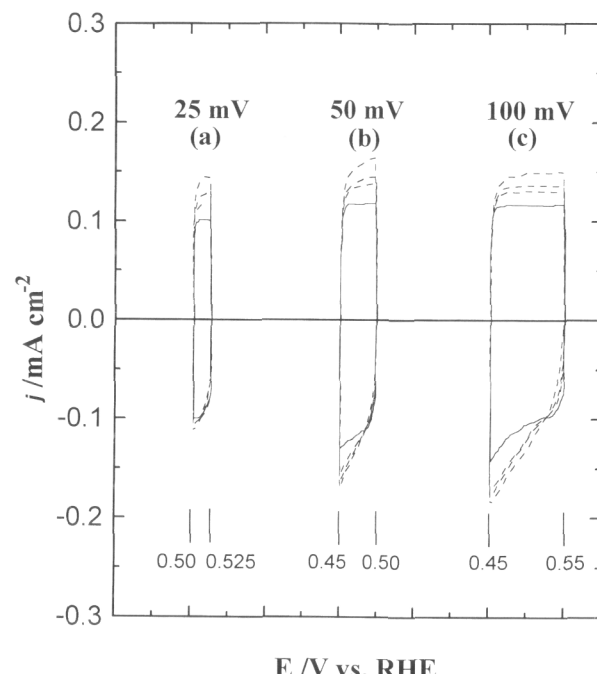


Fig. 6. CV responses (5 mVs^{-1}) in $1 \text{ M H}_2\text{SO}_4$ for an 80 nm thick PANI film, deposited on a Au quartz crystal substrate, scanned between (a) 0 and 0.6 V (—), (b) 0 and 0.45 V (· · ·), (c) multicycled between 0.425 and 0.450 V (---), (d) steady state response between 0.425 and 0.450 V (—), and then (e) scanned positively to 0.6 V (— · —).

due to water injection during multicycling between 0.425 and 0.450 V, some regions of the PANI film become more hydrated at this potential than they would in a normal CV scan. As a result, these sites can be oxidized at less positive potentials than usual. However, as these hydrated oxidized PANI sites are now stabilized, they cannot be reduced unless sufficiently negative potentials are applied.

Fig. 2 (curve d) shows that the reversible, steady-state current seen after ca. 20 cycles over the narrow range of potential, is significantly lower than that seen at the same potential in full range CVs. This is equivalent to an apparent decrease in PANI pseudo-capacitance. The steady-state mass-to-charge ratios are seen in Table 2 to be independent of sweep rate, at least up to 10 mVs^{-1} , for two different 25 mV potential ranges. At higher sweep rates, it was difficult to collect mass data accurately and reliably under these conditions. It can be seen that at potentials positive of ca. 0.45 V, i.e., when the film is fully conducting, the steady-state ratio is ca. $30 \text{ g}(\text{mol e}^-)^{-1}$. This is very similar to the value seen through most of the full negative scan (Table 1). This may be consistent with the fact that the magnitude of the steady-state anodic and cathodic currents in curve d (Fig. 2) are also very similar to the cathodic current passed in a normal full range CV when the potential is reversed at 0.45 V (Fig. 2, curve b). It therefore appears that the steady-state film capacitance is defined primarily by the inherently lower cathodic capacitance under these conditions.

To examine the impact of voltage amplitude on the CV response, a similar experiment to that of Fig. 2 was carried out using 50 and 100 mV amplitude scans. Fig. 7 shows that at 50 mV, excess anodic charge is again initially passed, but some film reduction can also now be achieved. For a 100 mV amplitude, the additional anodic charge passed is matched by an equivalent cathodic charge, so that no net film oxidation occurs under these conditions. These trends with voltage amplitude are correlated with the higher steady-state capacitances, also shown in Fig. 7, when the amplitude is increased from 25 to 100 mV. This shows that the reduced capacitance normally seen in a.c. impedance experiments depends strictly on the voltage amplitude and not on the frequency employed. In fact, the loss of pseudo-capacitance when only small voltage amplitudes are scanned is consistent with the UQR condition,



E/V vs. RHE

Fig. 7. CV responses (20 mVs^{-1}) in $1 \text{ M H}_2\text{SO}_4$ for a 70 nm thick PANI film, deposited on a Au quartz crystal substrate, scanned over three different voltage amplitudes: (a) 25 mV, (b) 50 mV, and (c) 100 mV. Both the responses leading to (---) and at (—) steady state are shown.

suggested above to originate from asymmetries in the water injection/expulsion process during oxidation/reduction of PANI films.

An important goal of this work was to establish the mass-to-charge ratio at steady-state in small voltage amplitude experiments. It was found that a ratio of ca. $30 \text{ g}(\text{mol e}^-)^{-1}$ was obtained for the three experiments shown in Fig. 7. This ratio is the same as that observed in the negative scan of a normal full potential range CV experiment (Table 1), where it was suggested that the charge compensation process involves a mixture of sulfate ion and water expulsion and some proton injection. It can therefore be concluded that no unusual reactions are occurring under the conditions of the small potential amplitude experiment and that the steady-state charge compensation process is the same as that which occurs during a normal reduction scan in a full potential range CV.

The results of Fig. 7 suggest that a potential window of at least 100 mV must be employed in order to reduce all of the sites which can be oxidized over this range of potential. When the amplitude is less than this, only the fraction of sites indicated in Fig. 1 (curve b) can be reversibly oxidized and reduced. These sites must not be susceptible to water transport limitations and/or are not susceptible to stabilization by hydration, exhibiting the same mass-to-charge ratio and lowered currents seen during the normal negative sweeps. In earlier studies of PANI, it has been suggested that the charge passed during PANI oxidation/reduction was composed of a faradaic and ca-

Table 2
Mass to charge ratio, determined during cycling within two different 25 mV intervals, as a function of sweep rate

Sweep rate/ mVs^{-1}	Steady-state mass-to-charge ratio/ $\text{g}(\text{mol e}^-)^{-1}$	
	0.475–0.500 V	0.525–0.550 V
2	29	30
5	29	30
10	30	33

PANI film (80 nm), deposited on a Au quartz crystal substrate, in $1 \text{ M H}_2\text{SO}_4$.

pacitive component [1,6,32]. Using this interpretation, our results might then have suggested that the steady-state capacitance obtained in small voltage amplitude experiments originates from double layer charging effects only. However, this cannot be the case, as it has been conclusively demonstrated by Kalaji and Peter [8] and Hutton et al. [33], using the frequency resolved transmittance technique, that all of the charge passed in PANI oxidation/reduction is faradaic in nature.

Although the local structural and/or chemical characteristics of the sites which respond reversibly over narrow potential ranges (Fig. 1, curve b) cannot be determined from the present work, a useful goal of future research would be to synthesize polymers in which a greater proportion of sites react reversibly. As an example, a more open polymer structure allowing more facile water injection, in particular, might be desirable. This would result in capacitively more efficient films.

4. Summary

Electrochemical and mass measurements have been carried out to further understand the loss of film capacitance in small voltage amplitude experiments (e.g., in a.c. impedance studies) vs. in full range CV cycles between the fully insulating and conducting film states. Only thin PANI films and slow sweep rates have been examined here, so that all PANI sites have sufficient time to react (all currents are linearly proportional to sweep rate under all conditions employed).

In full potential range CV experiments, it is noted that the principal redox peaks remain separated by ca. 100 mV, independent of sweep rate, and that the anodic currents at potentials more positive than the peaks are always larger than the corresponding cathodic ones. These results are characteristic of systems exhibiting unusual quasi reversibility (UQR), at least for some fraction of the film sites. It is also seen that the film mass increases nonlinearly during oxidation, from ca. 10 up to ca. 45 g(mol e⁻)⁻¹, while film reduction exhibits a steady-state 30 g(mol e⁻)⁻¹ ratio. This difference in the mass change, both with potential and direction of sweep, as well as an observed larger extent of hysteresis in the mass change with increasing sweep rate, suggests that water injection during PANI oxidation is hindered. In a normal CV experiment, it is seen that water injection occurs predominantly at higher potentials when the higher mass-to-charge ratios are seen, while water expulsion occurs more uniformly with potential during reduction. It is therefore proposed here that the origin of some of the asymmetries in the CV response of PANI and its UQR characteristics are related to delayed water injection during film oxidation.

When small voltage amplitudes are employed, it is seen that some PANI sites, normally not oxidizable until higher

potentials are reached, can initially react with time at lower potentials. The mass-to-charge ratio of ca. 40 g(mol e⁻)⁻¹, observed as these additional sites unexpectedly oxidize, is similar to that seen at high potentials during a full potential range positive scan, suggesting that sulfate and also water injection is occurring. Under these conditions, sufficient time has been allowed for the penetration of more water into PANI than would normally be present at the same potential in a typical CV scan, thus shifting the redox potential of the newly reacted sites negatively, so that they can now be oxidized. These sites, however, cannot be reduced without widening the potential window to more negative potentials, due to stabilization through site hydration.

The steady-state currents, observed in these narrow potential amplitude experiments after ca. 20 cycles, are significantly lower than those seen at the same potential in full range CVs, indicative of a loss in PANI pseudo-capacitance. However, they are similar in magnitude to the cathodic currents seen in a normal CV when the potential is reversed at potentials centered in the narrow voltage amplitude range under study. The mass-to-charge ratio at these steady-state conditions is ca. 30 g(mol e⁻)⁻¹, independent of voltage amplitude (ranging from 25 to 100 mV) and of sweep rate. Moreover, the ratio is similar to those seen in the normal full potential range negative scan. This ratio is considered to reflect a mixture of sulfate and water expulsion and some proton injection.

It appears that the sites yielding the steady-state pseudo-capacitance in small voltage amplitude experiments are those which are NOT susceptible to delays in water transport and/or those not stabilized by hydration effects. The charge compensating process associated with the reaction of these sites is the same as that for the sites reduced in the negative scan in a normal CV experiment, but not the same as that occurring in the positive scan. A goal of future research would be to synthesize new polymers having the advantageous properties of PANI, but which contain a greater fraction of sites which react reversibly, even when small voltage amplitudes are employed. This would yield capacitively more efficient films.

Acknowledgements

The authors are grateful to the Natural Sciences and Engineering Research Council of Canada (NSERC) for their overall support of this work. H.N. Dinh also acknowledges scholarship support from NSERC, Alberta Heritage Foundation, A.S.M. International ‘Calgary Chapter’, and the University of Calgary. The authors also wish to thank Dr. P. Vanýsek for access to a.c. impedance equipment and for useful discussions regarding impedance and QCMB experiments.

References

- [1] I. Rubinstein, E. Sabatani, *J. Electrochem. Soc.* 134 (1987) 3078.
- [2] M. Grzeszczuk, G. Zabinska-Olszak, *J. Electroanal. Chem.* 359 (1993) 161.
- [3] T. Komura, H. Sakabayashi, K. Takahashi, *Bull. Chem. Soc. Jpn.* 68 (1995) 476.
- [4] O. Genz, M.M. Lohrengel, J.W. Schultze, *Electrochim. Acta* 39 (1994) 179.
- [5] G. Sandi, P. Vanýsek, *Synth. Met.* 64 (1994) 1.
- [6] P. Fiordiponti, G. Pistoia, *Electrochim. Acta* 34 (1989) 215.
- [7] G. Inzelt, G. Láng, V. Kertész, J. Bácskai, *Electrochim. Acta* 38 (1993) 2503.
- [8] M. Kalaji, L.M. Peter, *J. Chem. Soc., Faraday Trans.* 87 (1991) 853.
- [9] X. Ren, P.G. Pickup, *J. Electroanal. Chem.* 372 (1994) 289.
- [10] G. Sauerbrey, *Z. Phys.* 155 (1955) 206.
- [11] A.A. Michri, A.G. Pshchenichnikov, R.Kh. Burshtein, *Sov. Elektrokhim.* 8 (1972) 351.
- [12] S. Gottesfeld, A. Redondo, S.W. Feldberg, *Electrochim. Soc. Extended Abstr.*, San Diego, CA, Abstract 507, (1986) 759.
- [13] D. Orata, D.A. Buttry, *J. Am. Chem. Soc.* 109 (1987) 3574.
- [14] H. Daifuku, T. Kawagoe, N. Yamamoto, T. Ohsaka, N. Oyama, *J. Electroanal. Chem.* 274 (1989) 313.
- [15] S. Cordoba-Torresi, C. Gabrielli, M. Keddam, H. Takenouti, R. Torresi, *J. Electroanal. Chem.* 290 (1990) 269.
- [16] C. Barbero, M.C. Miras, O. Haas, R. Kötz, *J. Electroanal. Chem.* 310 (1991) 437.
- [17] R.M. Torresi, S.I. Cordoba de Torresi, C. Gabrielli, M. Keddam, H. Takenouti, *Synth. Met.* 61 (1993) 291.
- [18] M.C. Miras, C. Barbero, R. Kötz, O. Haas, *J. Electroanal. Chem.* 369 (1994) 193.
- [19] S. Kuwabata, A. Kishimoto, H. Yoneyama, *J. Electroanal. Chem.* 377 (1994) 261.
- [20] B. Keita, A. Mahmoud, L. Nadjo, *J. Electroanal. Chem.* 386 (1995) 245.
- [21] C. Barbero, M.C. Miras, O. Haas, R. Kötz, *J. Electrochim. Soc.* 138 (1991) 669.
- [22] Desilvestro, W. Scheifele, O. Haas, *J. Electrochim. Soc.* 139 (1992) 2727.
- [23] S.W. Feldberg, I. Rubinstein, *J. Electroanal. Chem.* 240 (1988) 1.
- [24] B. Villeret, M. Nechtschein, *Phys. Rev. Lett.* 63 (1989) 1285.
- [25] J. Heinz, M. Störzbach, J. Mortensen, *Ber. Bunsenges. Phys. Chem.* 91 (1987) 960.
- [26] A. Redondo, E.A. Ticianelli, S. Gottesfeld, *Mol. Cryst. Liquid Cryst.* 160 (1988) 185.
- [27] J.Q. Chambers, F.B. Kaufman, K.H. Nichols, *J. Electrochim.* 142 (1982) 277.
- [28] G. Inzelt, L. Szabo, *Electrochim. Acta* 31 (1986) 1381.
- [29] P. Daum, R.W. Murray, *J. Am. Chem. Soc.* 65 (1981) 390.
- [30] C. Barbero, R. Kötz, *J. Electrochim. Soc.* 141 (1994) 859.
- [31] S.H. Glarum, J.H. Marshall, *J. Electrochim. Soc.* 134 (1987) 142.
- [32] K. Aoki, K. Hayashi, *J. Electroanal. Chem.* 384 (1995) 31.
- [33] R.S. Hutton, M. Kalaji, L.M. Peter, *J. Electroanal. Chem.* 270 (1989) 429.